



No discernible effect of Mg^{2+} ions on the equilibrium oxygen isotope fractionation in the CO_2 – H_2O system



Joji Uchikawa^{*}, Richard E. Zeebe¹

Department of Oceanography, SOEST, University of Hawaii at Manoa, 1000 Pope Road, Honolulu, HI 96822, USA

ARTICLE INFO

Article history:

Received 16 June 2012

Received in revised form 31 January 2013

Accepted 7 February 2013

Available online 15 February 2013

Editor: U. Brand

Keywords:

Oxygen isotopes

Mg^{2+} ions

Carbonate chemistry

$\delta^{18}O$ paleothermometry

ABSTRACT

Equilibrium oxygen isotope fractionation factors ($\alpha_{CO_2(g)-H_2O}$, $\alpha_{HCO_3-H_2O}$ and $\alpha_{CO_3-H_2O}$) are fundamental geochemical parameters that characterize ^{18}O partitioning in the CO_2 – H_2O system. These constants were established in laboratory experiments using deionized H_2O (e.g., Beck et al. (2005) and references therein). The applicability of these constants in environmental waters, including natural seawater, appears questionable due to potentially strong ionic interactions in such aqueous media. For instance, considerable portions of carbonate ions in seawater exist as cation– CO_3^{2-} ion complexes such as $MgCO_3^0$. In this study, quantitative $BaCO_3$ precipitation experiments were performed to examine the effect of Mg^{2+} concentrations on the oxygen isotope equilibrium between dissolved inorganic carbon (DIC) species and H_2O . Our results from Mg^{2+} -free control experiments in which $BaCO_3$ samples were precipitated from simple $NaHCO_3$ solutions were in good agreement with empirical results from three independent studies and with theoretical calculations. $BaCO_3$ precipitations from solutions with Mg^{2+} concentrations higher than 2.5 mM caused intolerable quantities of $Mg(OH)_2$ co-precipitation, which interfered with $\delta^{18}O$ measurements. Within the limit of 2.5 mM of $[Mg^{2+}]$, the $MgCO_3^0$ abundance in the total carbonate ions ($[CO_3^{2-}]_T$) and [DIC] was varied over approximately 0 to 40% and 0 to 36%, respectively, by manipulating solution chemistry. Despite such chemical treatment, there was no effect of Mg^{2+} -addition on $\alpha_{BaCO_3-H_2O}$. These results suggest that the presence of Mg^{2+} in solutions has a negligible effect on the oxygen isotope equilibrium in the CO_2 – H_2O system. In seawater, Mg^{2+} is the most important cation that forms complexes with CO_3^{2-} . Hence, if our results also hold at higher $[Mg^{2+}]$ and higher ionic strength, they imply that the applicability of freshwater-based equilibrium fractionation factors is not compromised by ionic interactions in seawater.

© 2013 Elsevier B.V. All rights reserved.

1. Introduction

Stable oxygen and carbon isotope ($\delta^{18}O$ and $\delta^{13}C$) values of marine biogenic carbonates such as foraminiferal tests are fundamental tools to study the climatic history of the Earth. The $\delta^{18}O$ values of biogenic carbonates reflect the temperatures and the ^{18}O content of seawater in which these carbonates were formed (Urey, 1947; McCrea, 1950; Epstein et al., 1953; Grossman and Ku, 1986; Bemis et al., 1998), hence they are useful for reconstructions of past changes in seawater temperatures, hydrological cycles and global ice volumes over various timescales (e.g., Zachos et al., 2001; Oppo et al., 2003; Lisiecki and Raymo, 2005; Cramer et al., 2009; Friedrich et al., 2012). On the other hand, $\delta^{13}C$ values of biogenic carbonates can be used to elucidate past changes in large-scale ocean circulation, biogeochemical processes and global carbon cycling (e.g., Curry et al., 1988; Dickens et al., 1995; Kennett et al., 2000; Cramer et al., 2009;

Friedrich et al., 2012). Collectively, $\delta^{18}O$ and $\delta^{13}C$ values of biogenic carbonates can provide important clues to unravel the nature of past climate changes in response to various forcing mechanisms including atmospheric CO_2 concentrations. Particularly, the information obtained from past hyperthermal events (such as the Paleocene–Eocene thermal maximum) have important implications for the realistic prediction of the climatic fate of the ongoing anthropogenic carbon emissions (Zachos et al., 2008).

The theoretical basis of the paleoceanographic utility of $\delta^{18}O$ and $\delta^{13}C$ values of biogenic carbonates relies on oxygen and carbon isotope partitioning in the CO_2 – $CaCO_3$ – H_2O system. Isotope effects that regulate the partitioning have been quantified in deionized H_2O (e.g., McCrea, 1950; Halas and Wolacewicz, 1982; Brenninkmeijer et al., 1983; Mook, 1986; Romanek et al., 1992; Kim and O'Neil, 1997; Beck et al., 2005; Kim et al., 2006). Among the list, McCrea (1950), Beck et al. (2005) and Kim et al. (2006) are of particular relevance to this study. Beck et al. (2005) comprehensively quantified the equilibrium oxygen isotope fractionation factors of dissolved inorganic carbon (DIC) species with respect to H_2O ($\alpha_{CO_2(aq)-H_2O}$, $\alpha_{HCO_3-H_2O}$ and $\alpha_{CO_3-H_2O}$) in freshwater, based on an acid-stripping method and quantitative inorganic carbonate precipitation experiments. Their

^{*} Corresponding author. Tel.: +1 808 956 3285; fax: +1 808 956 7112.

E-mail addresses: uchikawa@hawaii.edu (J. Uchikawa), zeebe@soest.hawaii.edu (R.E. Zeebe).

¹ Tel.: +1 808 956 6473; fax: +1 808 956 7112.

experimental results were verified by Kim et al. (2006) who performed similar carbonate precipitation experiments. Furthermore, the results from these studies are also in agreement with the classic work of McCrea (1950) (see Usdowski and Hoefs (1993) for the correction on McCrea's data). But the fractionation factors determined in freshwater may not be directly applicable to seawater, which contains numerous ionic species that may influence isotopic fractionation by forming ion complexes with DIC species.

For instance, Thode et al. (1965) showed that the equilibrium carbon isotope fractionation between DIC and gaseous CO_2 increases with Mg^{2+} concentrations in solutions (Fig. 1). Zhang et al. (1995) also documented that the use of seawater rather than deionized H_2O as the aqueous media results in apparent offsets in the equilibrium carbon isotope fractionation between DIC and gaseous CO_2 . Their experimental results further indicate that the magnitude of the offset increases with the proportion of CO_3^{2-} ions in the CO_2 - H_2O system. The experimental condition of Zhang et al. (1995) was purely inorganic whereas Thode et al. (1965) used carbonic anhydrase in their experiments. Because this enzyme has a sizable kinetic carbon isotope effect on CO_2 hydration and its reverse reaction (Paneth and O'Leary, 1985), a direct qualitative comparison of the experimental data from these independent studies is inappropriate. However, these data concurrently imply that the complex formation between Mg^{2+} and CO_3^{2-} as MgCO_3^0 affects equilibrium carbon isotope fractionation between CO_3^{2-} and gaseous CO_2 , presumably due to the enrichment of ^{13}C in MgCO_3^0 complexes (Thode et al., 1965; Zhang et al., 1995). We emphasize that it is not our intention to re-evaluate the effect of Mg^{2+} on the carbon isotope equilibrium in the CO_2 - H_2O system in this paper. Rather, our main goal is to evaluate if the presence of Mg^{2+} in solutions likewise affects ^{18}O equilibrium in the CO_2 - H_2O system by forming MgCO_3^0 complexes.

Beck et al. (2005) argued that the effect of ion pairs on the ^{18}O equilibrium is negligible based on the results from a set of experiments in which the relative abundance of NaCO_3^- complexes was varied from 18 to 45% in [DIC]. This conclusion, however, does not take into account the results of Thode et al. (1965) who found that only Mg^{2+} had a

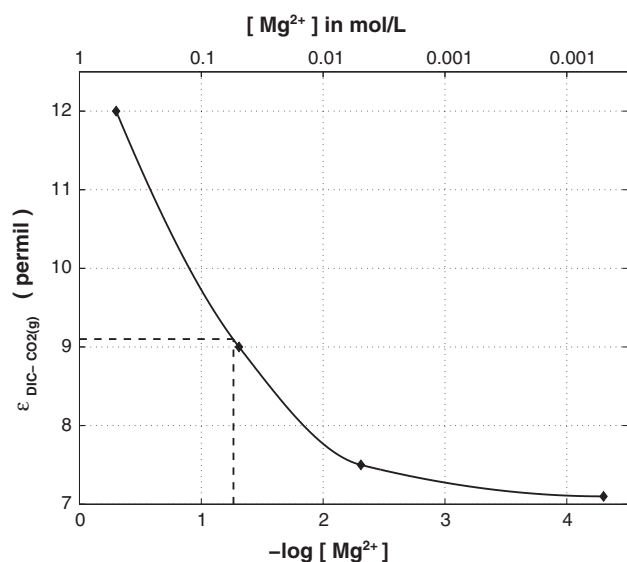


Fig. 1. Dependence of the equilibrium carbon isotope fractionation between DIC and gaseous CO_2 ($\epsilon_{\text{DIC-CO}_2(\text{g})}$) on $[\text{Mg}^{2+}]$ in solutions established by Thode et al. (1965). These experiments were conducted at 25 °C and pH 7.9 with constant $[\text{Na}^+]$ of 24.8 mM and variable $[\text{Mg}^{2+}]$. The dashed lines in the panel indicate the typical seawater $[\text{Mg}^{2+}]$ of 53 mmol/kg (~54 mM) and corresponding $\epsilon_{\text{DIC-CO}_2(\text{g})}$ value of 9.1‰. Note that this reflects ^{13}C enrichment of nearly 2‰ in comparison to the Mg^{2+} -free condition. The reporting of the fractionation factor in ϵ notation is related to α by $\epsilon = (\alpha - 1) \times 1000$.

marked influence on the equilibrium carbon isotope fractionation among a suite of cations (Mg^{2+} , Fe^{2+} , Co^{2+} , Ni^{2+} , Al^{3+} and Cr^{3+}). Given the observations of Thode et al. (1965) and the fact that MgCO_3^0 is the most dominant form of cation- CO_3^{2-} complexes in seawater (Garrels and Thompson, 1962; Kester and Pytkowicz, 1969; Pytkowicz and Hawley, 1974; Siebert and Hostetler, 1997b), we performed quantitative BaCO_3 precipitation experiments in the presence of Mg^{2+} to address if freshwater-based $\alpha_{\text{CO}_2(\text{aq})-\text{H}_2\text{O}}$, $\alpha_{\text{HCO}_3-\text{H}_2\text{O}}$ and $\alpha_{\text{CO}_3-\text{H}_2\text{O}}$ hold in environmental waters including seawater. This has important implications for various applications in aquatic stable isotope geochemistry. For example, the applicability of $\alpha_{\text{CO}_2(\text{aq})-\text{H}_2\text{O}}$, $\alpha_{\text{HCO}_3-\text{H}_2\text{O}}$ and $\alpha_{\text{CO}_3-\text{H}_2\text{O}}$ in seawater is crucial to unraveling the underlying mechanism(s) of $\delta^{18}\text{O}$ vital effects (e.g., Spero et al., 1997; Zeebe, 1999; Adkins et al., 2003; McConnaughey, 2003; Rollion-Bard et al., 2003; Zeebe, 2007; Allison et al., 2010).

In this study, a series of quantitative BaCO_3 precipitation experiments analogous to those of Beck et al. (2005) were performed. However, we incorporated Mg^{2+} in the parent NaHCO_3 solutions to determine if equilibrium oxygen isotope fractionation in the CO_2 - H_2O system will be affected in a similar fashion as observed for carbon isotopes (Thode et al., 1965; Zhang et al., 1995). The ultimate goal of the present study is to shed light on the fidelity of the $\alpha_{\text{CO}_2(\text{aq})-\text{H}_2\text{O}}$, $\alpha_{\text{HCO}_3-\text{H}_2\text{O}}$ and $\alpha_{\text{CO}_3-\text{H}_2\text{O}}$ values established by Beck et al. (2005) in natural waters, particularly in seawater.

2. Methods

2.1. Experimental designs

Quantitative carbonate precipitation refers to a quasi-instantaneous and complete transformation of DIC into solid carbonate minerals. The $\delta^{18}\text{O}$ values of carbonates quantitatively precipitated from HCO_3^- and/or CO_3^{2-} dominated solutions reflect the overall $\delta^{18}\text{O}$ values of DIC. Accordingly, if the parent solutions (from which the carbonates are formed) are fully equilibrated, the $\delta^{18}\text{O}$ values of the resultant carbonates can be used to infer equilibrium oxygen isotope fractionation in the carbonic acid system (McCrea, 1950; Zeebe, 1999; Beck et al., 2005; Kim et al., 2006; Zeebe, 2007; Uchikawa and Zeebe, 2012). General procedures for quantitative BaCO_3 precipitations were modified from Beck et al. (2005).

During the first phase of the study, we performed a series of control experiments by replicating the “equilibration experiments” of Beck et al. (2005). In these control experiments, samples were quantitatively precipitated from 15 mM NaHCO_3 solutions prepared at various pH levels. To test the reliability of our protocols for the precipitation experiments, the outcomes from the control experiments were compared to the empirical data from McCrea (1950), Beck et al. (2005) and Kim et al. (2006), in which the precipitations were performed from simple Na^+ - CO_2 - H_2O systems.

In the second phase, we performed experiments using the 15 mM NaHCO_3 solutions containing variable amounts of Mg^{2+} (referred to as the “variable $[\text{Mg}^{2+}]$ experiments”). The Mg^{2+} concentrations tested in these experiments ranged from 2.8 μM to 106.4 mM. Note that typical seawater $[\text{Mg}^{2+}]$ is approximately 54 mM. Finally, in the third phase, experiments were performed using the parent solutions prepared at constant $[\text{Mg}^{2+}]$ of 2.5 mM but variable [DIC] ranging from 1.9 to 15 mM (referred to as the “constant $[\text{Mg}^{2+}]$ experiments”).

2.2. Preparation and ^{18}O equilibration of the parent solutions

The parent NaHCO_3 solutions were prepared in serum bottles sealed with rubber stoppers and aluminum crimps. Although the NaHCO_3 powder used for the experiments (certified A.C.S. grade, Fisher #S233-500) was not isotopically labeled, its $\delta^{13}\text{C}$ and $\delta^{18}\text{O}$ values were homogeneous ($\delta^{13}\text{C}_{\text{VPDB}} = -2.89 \pm 0.02\text{‰}$ and $\delta^{18}\text{O}_{\text{VPDB}} = -15.81 \pm 0.10\text{‰}$, $n = 13$). The NaHCO_3 powder was placed in serum

bottles, which were subsequently evacuated and pressurized with N₂ gas. Then, CO₂-free deionized H₂O was introduced into the bottles using disposable clinical syringes. Care was taken to minimize the headspace in the bottles. Deionized H₂O was continuously bubbled with N₂ gas for a minimum of one week in a large carboy for removal of residual dissolved CO₂ prior to use. Aliquots of H₂O used for the preparations of the parent solutions were sampled for δ¹⁸O measurements. The pH of parent solutions was adjusted with NaOH solutions prepared from low-carbonate reagent A.C.S. grade NaOH pellets (J.T. Baker #3722). Also, variable amounts of MgCl₂ solution prepared from certified A.C.S. grade MgCl₂·6H₂O (Fisher #M33-500) were added to adjust [Mg²⁺] in the parent solutions. The NaOH and MgCl₂ solutions were similarly prepared from CO₂-free deionized H₂O.

The parent solutions were kept at 25 ± 0.04 °C in water baths equipped with immersion circulators (Thermo Scientific HAAKE C10 and SC100 models) for a period of a few days up to several months to ensure that the CO₂-H₂O system reached ¹⁸O equilibrium. It should be noted that ¹⁸O equilibration time depends on the abundance of CO_{2(aq)} relative to other DIC species, which depends on solution pH (Table 1). This is because direct exchange of oxygen isotopes between DIC species and H₂O only occurs via hydration and hydroxylation of CO₂ (see Zeebe and Wolf-Gladrow, 2001; Uchikawa and Zeebe, 2012).

2.3. Quantitative carbonate precipitations

Once equilibrated, 20 mL of the parent solutions was withdrawn from serum bottles and transferred into serum vials containing excess reagent grade BaCl₂·2H₂O (J.T. Baker #0974) under N₂-atmosphere. Addition of the parent solutions led to complete dissolution of the BaCl₂·2H₂O within a few seconds. This step was immediately followed by addition of 2.5 M NaOH solution to trigger instantaneous BaCO₃ precipitation. From each parent solution, BaCO₃ precipitation was performed in duplicate. The precipitates were immediately vacuum-filtered onto 0.2 μm cellulose-nitrate membrane filters and rinsed with a generous volume of CO₂-free deionized H₂O. Filtration of the samples from the control experiments and the variable [Mg²⁺] experiments was conducted in ambient atmosphere. Special care was taken to minimize sample contamination from absorption of ambient CO₂ by immediately diluting the precipitate-solution mixtures by CO₂-free deionized H₂O upon filtration. For the samples from the constant [Mg²⁺] experiments, filtration was performed under N₂-atmosphere using disposable glove bags. The samples were then oven dried overnight at 65 °C, weighed and stored in air-tight glass vials until subsequent analyses.

The remainder of the parent solutions was allocated for pH measurements, which were performed by either a benchtop pH meter (Thermo Scientific Orion 3-Star Plus model) or by the auto-titrator system of Zeebe and Sanyal (2002). These systems were equipped with an Orion triode combination pH electrode (Thermo Scientific #9157BNMD) and an Orion sure-flow pH electrode (Thermo Scientific #8272BN), respectively. The electrodes were calibrated on a daily basis using Orion pH buffers (pH 4.01, 7.00, 10.01) that are traceable to NIST standard reference materials.

Table 1

The time required for 99% completion of ¹⁸O equilibrium in the carbonic acid system (denoted as t_{99%}) at 25 °C and 0 salinity (Zeebe and Wolf-Gladrow, 2001; Uchikawa and Zeebe, 2012). Calculations are based on freshwater constants (see Uchikawa and Zeebe, 2012).

pH	7.5	8	8.5	9	9.5	10	10.5	11	11.5	12	12.5
t _{99%} (h)	2.0	5.1	10.4	16.1	21.0	28.6	49.3	113.8	317.1	960.0	2993.1

2.4. Characterization of the solution chemistry

Interactions of the dissolved ionic species in the parent solutions were modeled by a scheme similar to that of Garrels and Thompson (1962) (see Appendix A). We particularly focused on the abundance of MgCO₃⁰ complexes relative to the total DIC and CO₃²⁻ ion concentration in the parent solutions (denoted as [DIC] and [CO₃²⁻]_T, respectively), as these seem to be the most important parameters based on the experimental results by Thode et al. (1965) and Zhang et al. (1995) (Fig. 1).

Our calculations for the ionic interactions represent a simplified model based on a few assumptions. This model provides reasonable approximations for the activities and concentrations of various ion complexes in the parent solutions without employing an iterative scheme, unlike other more sophisticated speciation models. For example, our estimates for the MgCO₃⁰ abundance relative to [DIC] and [CO₃²⁻]_T and those estimates by WEB-PHREEQ (the online version of the PHREEQC aqueous geochemical model by Parkhurst and Appelo (1999)) generally agreed within 5%. Disagreements of about 10 to 15% were only found for the parent solutions with very high [Mg²⁺] and/or pH (>~10), where the WEB-PHREEQ failed to converge within the prescribed iteration cycles.

2.5. Sample mineralogy

In this study, samples were precipitated as BaCO₃ rather than CaCO₃, as the latter can form different types of polymorphs. Our preliminary samples quantitatively precipitated as CaCO₃ from simple NaHCO₃ solutions always resulted in co-precipitation of calcite and variable amounts of vaterite (Uchikawa and Zeebe, 2012). Co-precipitation of calcite and vaterite was similarly observed under relatively rapid inorganic CaCO₃ precipitations in previous studies (e.g., Kim and O'Neil, 1997; Kim et al., 2006). Aragonite precipitation is also possible when Mg²⁺ is present in the parent solutions (Morse et al., 1997; Kim et al., 2007b). Inhomogeneous sample mineralogy interferes with the δ¹⁸O measurements of carbonate samples due to the mineral-specific acid fractionation factors (AFF), as summarized in Kim et al. (2007a).

On the contrary, BaCO₃ precipitates only in orthorhombic orientation as witherite. Successful witherite synthesis from solutions with simple Na⁺-CO₂-H₂O system via quantitative precipitation has been confirmed in previous studies (Beck et al., 2005; Kim et al., 2006; Uchikawa and Zeebe, 2012), but not from the solutions containing Mg²⁺. For the characterization of the sample mineralogy by X-ray diffraction (XRD) analyses, we prepared additional representative samples from the solutions with [DIC] of 15 mM and variable [Mg²⁺]. These samples were sent to the University of Hawaii at Hilo XRD facility for the analyses.

2.6. Stable isotope analyses

The BaCO₃ and H₂O samples were sent to the University of California Davis stable isotope laboratory for δ¹⁸O and δ¹³C measurements.

Isotopic analyses of the BaCO₃ samples were conducted by traditional acid digestion where samples were reacted with supersaturated H₃PO₄ (specific gravity = 1.93 g/cm³) *in vacuo* to produce CO₂ gas. The acid digestion of the samples was performed at 90 °C using an ISOCARB common acid bath auto-carbonate device. The resultant CO₂ gas was analyzed by a Micromass Optima isotope ratio mass spectrometer (IRMS). An in-house calcite standard calibrated to NBS-19 reference material was simultaneously analyzed with the samples. Instrument precisions for δ¹⁸O and δ¹³C analyses based on repeat analyses of the in-house standard were ± 0.05‰ and ± 0.04‰, respectively. The δ¹⁸O values of the H₂O samples were determined by the conventional CO₂-H₂O equilibration method (Epstein and Mayeda, 1953). An automated equilibrator attached to a Finnigan MAT 251 IRMS was used for the analyses. Instrument precision was ± 0.03‰.

The stable isotope data are reported in δ notation, expressed in permil (‰):

$$\delta = \left(\left(R_{\text{Sample}} / R_{\text{Standard}} \right) - 1 \right) \times 1000 \quad (1)$$

where R is the isotope ratio $^{18}\text{O}/^{16}\text{O}$ (denoted as ^{18}R) or $^{13}\text{C}/^{12}\text{C}$. The $\delta^{18}\text{O}$ and $\delta^{13}\text{C}$ data for the BaCO_3 samples are reported in VPDB, whereas the $\delta^{18}\text{O}$ data for H_2O samples are in VSMOW. However, the $\delta^{18}\text{O}$ values of the BaCO_3 samples are also re-scaled to VSMOW in order to calculate the fractionation factor:

$$\alpha_{\text{BaCO}_3\text{-H}_2\text{O}} = \left(\delta^{18}\text{O}_{\text{BaCO}_3} + 1000 \right) / \left(\delta^{18}\text{O}_{\text{H}_2\text{O}} + 1000 \right). \quad (2)$$

The formulation of Coplen et al. (1983) was used for conversion from VPDB to VSMOW scale:

$$\delta^{18}\text{O}_{\text{VSMOW}} = 1.0391 \times \delta^{18}\text{O}_{\text{VPDB}} + 30.91\text{‰}. \quad (3)$$

For our BaCO_3 $\delta^{18}\text{O}$ data, no correction was made to account for the difference between the BaCO_3 and calcite AFF. The primary reason for the decision is the fact that the BaCO_3 AFF is not well-established in comparison to the calcite AFF. Sharma and Clayton (1965) and Kim and O'Neil (1997) represent the only studies in which the BaCO_3 AFF was determined at 25 °C by directly analyzing the $\delta^{18}\text{O}$ of the total oxygen content in BaCO_3 . But there is a disparity of 0.34‰ for the AFF from these studies as opposed to only 0.05‰ of inconsistency in the calcite AFF from the literature (Sharma and Clayton, 1965; Das Sharma et al., 2002; Kim et al., 2007a). Böttcher (1996) published an expression for the temperature dependence of the BaCO_3 AFF between 20 and 90 °C, but his work entirely depends on the normalization to the BaCO_3 AFF by Sharma and Clayton (1965). The use of the BaCO_3 AFF (although conceptually proper) will lead to greater uncertainty in $\delta^{18}\text{O}$ values. Also note that the use of the calcite AFF for our BaCO_3 samples simply causes a constant offset from their “true” $\delta^{18}\text{O}$ values. It does not compromise the trends/patterns in our experimental results. Our data interpretations will not be biased irrespective of the use of the BaCO_3 or calcite AFF.

3. Results

3.1. XRD data

The XRD profile of the sample precipitated from a simple NaHCO_3 solution devoid of Mg^{2+} is highly consistent with the expected pattern for witherite (BaCO_3), as shown in Fig. 2. The same is also true for the samples produced from the solutions containing up to 2.5 mM of Mg^{2+} . Their XRD profiles are indistinguishable from one another. Unfortunately the XRD scanning for the samples from the solutions containing 26.6 and 53.2 mM of Mg^{2+} was limited to diffraction angles (2θ) below 40°. Therefore the characteristic clustering peaks between 40° and 50° are not verifiable in these truncated profiles. Nonetheless, other major BaCO_3 reference peaks (roughly at 23°, 27° and 34°) are well-resolved in these profiles. However, these particular profiles also exhibit peaks at 2θ of ~17° and ~38°, which separates them from the XRD profiles for the rest of the samples. These signals align with the characteristic reference peaks of brucite ($\text{Mg}(\text{OH})_2$).

3.2. Control experiments and error estimates

The data from the control experiments are summarized in Table S1 (Supplementary materials). The sample yield ranged from 96.6% to 103.9% with an average of $100.3 \pm 1.3\%$ ($n=70$) relative to the expected yield (Table 2). The expected yield was calculated stoichiometrically, assuming complete transformation of DIC into BaCO_3 . The

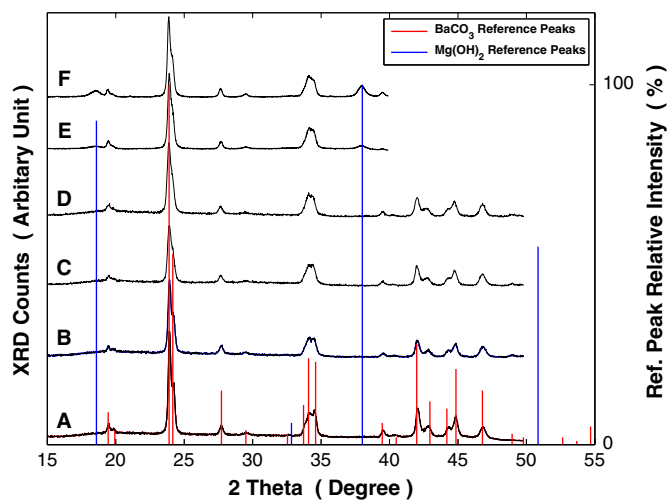


Fig. 2. XRD patterns of the samples quantitatively precipitated from 15 mM NaHCO_3 solutions with variable $[\text{Mg}^{2+}]$. (A) No Mg^{2+} present, (B) $[\text{Mg}^{2+}] = 25 \mu\text{M}$, (C) $[\text{Mg}^{2+}] = 250 \mu\text{M}$, (D) $[\text{Mg}^{2+}] = 2.5 \text{ mM}$, (E) $[\text{Mg}^{2+}] = 26.6 \text{ mM}$ and (F) $[\text{Mg}^{2+}] = 53.2 \text{ mM}$. Four replicate samples were prepared at each $[\text{Mg}^{2+}]$ level. The XRD patterns of the replicate samples were virtually indistinguishable. The reference peaks are from JCPDS (Joint Committee on Powder Diffraction Standards, 1974) file 5-378 for BaCO_3 (synthetic witherite) in red and file 7-239 for $\text{Mg}(\text{OH})_2$ (synthetic brucite) in blue.

$\delta^{13}\text{C}_{\text{BaCO}_3}$ values of the samples from the control experiments ranged from -3.68‰ to -2.84‰ with an average of $-3.16 \pm 0.14\text{‰}$. The $\delta^{13}\text{C}_{\text{BaCO}_3}$ values of the majority of the samples produced from the control experiments agreed with the $\delta^{13}\text{C}$ value of the NaHCO_3 used for the experiments ($-2.89 \pm 0.02\text{‰}$, $n=13$) within $\pm 0.5\text{‰}$. These stoichiometric and isotopic constraints validate successful quantitative precipitations.

Fig. 3 compares the $\alpha_{\text{BaCO}_3\text{-H}_2\text{O}}$ data based on the Mg^{2+} -free control experiments from this study and those from McCrea (1950), Beck et al. (2005) and Kim et al. (2006). Our $\alpha_{\text{BaCO}_3\text{-H}_2\text{O}}$ data obtained from the control experiments are in good agreement with these independent results over the entire pH range, which supports the reliability of our experimental protocols. Also shown in the figure is $\alpha_{\text{S-H}_2\text{O}}$, which is defined as the overall equilibrium oxygen isotope fractionation between S and H_2O (where $\text{S} = [\text{CO}_2(\text{aq})] + [\text{H}_2\text{CO}_3] + [\text{HCO}_3^-] + [\text{CO}_3^{2-}]$) from Zeebe (2007). Note that $\alpha_{\text{BaCO}_3\text{-H}_2\text{O}}$ and $\alpha_{\text{S-H}_2\text{O}}$ should be identical when BaCO_3 samples are quantitatively precipitated from fully equilibrated solutions.

We statistically evaluate two types of errors for the results from the control experiments: (1) typical experimental reproducibility at

Table 2
Description of the experimental conditions and brief summary of the results.

	[DIC]	$[\text{Mg}^{2+}]$	n	Average yield (weight %)	Average $\delta^{13}\text{C}$ (‰, VPDB)	Data display
Control experiments	15 mM	0	70	100.3 ± 1.3	-3.16 ± 0.14	Fig. 3
Variable $[\text{Mg}^{2+}]$ experiments	15 mM	2.78 μM	33	99.8 ± 1.2	-3.23 ± 0.22	Fig. 4
	15 mM	27.8 μM	34	100.0 ± 1.5	-3.19 ± 0.24	Fig. 4
	15 mM	278 μM	38	100.3 ± 1.3	-3.30 ± 0.30	Fig. 4
	15 mM	2.5 mM	31	103.8 ± 3.2	-3.30 ± 0.12	Fig. 4
	15 mM	26.6 mM	27	129.1 ± 4.0	-3.15 ± 0.22	Fig. 5
	15 mM	53.2 mM	27	162.5 ± 16.7	-3.09 ± 0.22	Fig. 5
	15 mM	106.4 mM	12	142.8 ± 21.4	-2.93 ± 0.33	Fig. 5
Constant $[\text{Mg}^{2+}]$ experiments	15 mM	2.5 mM	8	108.4 ± 3.1	-3.29 ± 0.11	Fig. 6
	7.44 mM	2.5 mM	8	115.0 ± 8.8	-3.55 ± 0.06	Fig. 6
	3.75 mM	2.5 mM	7	121.9 ± 3.5	-3.57 ± 0.14	Fig. 6
	1.86 mM	2.5 mM	8	144.4 ± 9.6	-4.19 ± 0.40	N/A

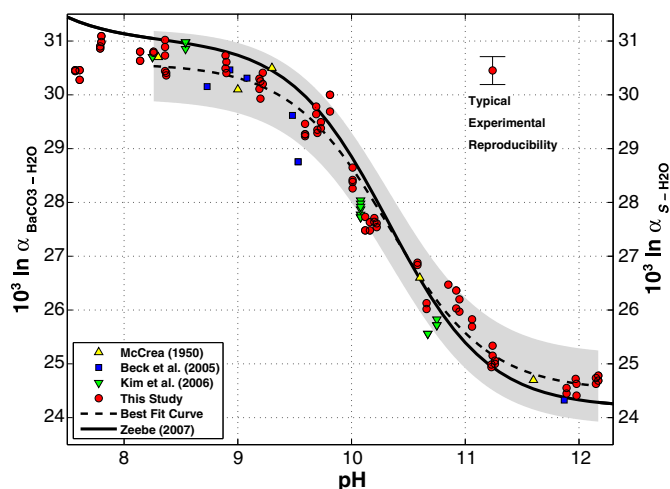


Fig. 3. Compilation of the empirical α_{S-H_2O} data at 25 °C based on the experiments in $Na^+-CO_2-H_2O$ system devoid of Mg^{2+} . Note that the fractionation factor α is expressed in the form of $10^3 \ln \alpha$. (Yellow upward triangles) Data from McCrea (1950). The data presented here are re-calculated values by Usdowski and Hoefs (1993). (Blue squares) Original data from Beck et al. (2005). Note that their isotopic measurements on the $BaCO_3$ samples are based on calcite AFF of $10^3 \ln \alpha_{CO_2-CaCO_3} = 8.12$ at 70 °C, which slightly contradicts with published calcite AFF values of about 8.65 at 70 °C (e.g., Das Sharma et al., 2002; Kim et al., 2007a). No corrections for $BaCO_3$ AFF were made. See Section 2.6. (Green downward triangles) Data from Kim et al. (2006). Their original data are based on $BaCO_3$ AFF of Kim and O'Neil (1997). The data presented here are recalculated with calcite AFF of Das Sharma et al. (2002). See Section 2.6. (Red circles) The results from the control experiment in the present study. Typical experimental reproducibility (± 0.26 in $10^3 \ln \alpha_{BaCO_3-H_2O}$) represents the average 2σ standard deviation of replicate experiments at a given pH. (Dashed curve) Nonlinear least squares fitting of the results from the control experiments to Eq. (4) as a function of pH ($r^2 = 0.98$). The shaded region indicates the 95% confidence interval for predictions based on the statistical fit. See Section 3.2 for details. (Solid curve) Theoretical α_{S-H_2O} values (where $S = [CO_{2(aq)}] + [H_2CO_3] + [HCO_3^-] + [CO_3^{2-}]$) as a function of pH by Zeebe (2007).

a given pH and (2) deviation of the experimental results from a best fit curve as a function of pH, where the mathematical expression for the best fit curve is based on Zeebe (2007). Based on the average 2σ standard deviation of our replicate experiments, typical experimental reproducibility at a given pH is about ± 0.26 in $10^3 \ln \alpha_{BaCO_3-H_2O}$. This compares well with the standard error reported in Beck et al. (2005). Above pH 8.2, the sum of $[CO_{2(aq)}]$ and $[H_2CO_3]$ accounts for less than 1% of the total DIC at 25 °C (Zeebe and Wolf-Gladrow, 2001). In that case, the mathematical expression of α_{S-H_2O} in Zeebe (2007) can be simplified to:

$$\alpha_{S-H_2O} = \frac{r_{CO_3^{2-}} + (r_{HCO_3^-} - r_{CO_3^{2-}}) \cdot X_{HCO_3^-}}{1 - r_{CO_3^{2-}} + (r_{CO_3^{2-}} - r_{HCO_3^-}) \cdot X_{HCO_3^-}} \cdot \frac{1}{18R_{H_2O}} \quad (4)$$

where $X_{HCO_3^-}$ is the mole fraction of HCO_3^- in the total DIC and $r_{HCO_3^-}$ and $r_{CO_3^{2-}}$ depend on the equilibrium oxygen isotope fractionation factor $\alpha_{HCO_3-H_2O}$ and $\alpha_{CO_3-H_2O}$, respectively. By fitting the results from our control experiments to this expression (Eq. (4)) using the nonlinear least squares approach (dashed curve in Fig. 3; $r^2 = 0.98$), we obtain $10^3 \ln \alpha_{HCO_3-H_2O} = 30.58 \pm 0.12$ and $10^3 \ln \alpha_{CO_3-H_2O} = 24.50 \pm 0.14$ in comparison to the respective value of 31.00 ± 0.15 and 24.19 ± 0.26 by Beck et al. (2005) at 25 °C. The 95% confidence interval for predictions based on our curve fitting is roughly ± 0.65 in $10^3 \ln \alpha_{BaCO_3-H_2O}$ (shaded region in Fig. 3), which encapsulates most of the existing experimental data (from McCrea (1950), Beck et al. (2005), Kim et al. (2006) and this study). Note that the theoretical curve of α_{S-H_2O} (Zeebe, 2007) shown in Fig. 3 relies on Beck et al.'s (2005) temperature-dependent expression of $\alpha_{HCO_3-H_2O}$ and $\alpha_{CO_3-H_2O}$ over the range of 15 °C to 40 °C. Using all data now available at 25 °C, one

could revise the theoretical curve using best fit results. But this theoretical curve would be limited to a single temperature.

The data compilation of independent quantitative carbonate precipitation experiments is largely consistent with Zeebe's (2007) theoretical α_{S-H_2O} as a function of pH (Fig. 3). The only exception is our $\alpha_{BaCO_3-H_2O}$ data at pH ~7.6. When $CO_{2(aq)}$ undergoes hydration and/or hydroxylation reaction, the resultant HCO_3^- (and CO_3^{2-} from deprotonation of HCO_3^-) is initially depleted in ^{18}O (see McConnaughey, 2003; Rollion-Bard et al., 2003; Beck et al., 2005). Upon quantitative precipitation, these ^{18}O -depleted HCO_3^- and CO_3^{2-} are instantaneously incorporated into $BaCO_3$ without reaching ^{18}O equilibrium with H_2O . It is most likely that the abundance of $CO_{2(aq)}$ was significant enough at pH ~7.6 to leave an ^{18}O -depleted signal in S.

3.3. Variable $[Mg^{2+}]$ experiments

The data from the variable $[Mg^{2+}]$ experiments are summarized in Table S2 (Supplementary materials). In these experiments, $BaCO_3$ precipitations were performed from the parent $NaHCO_3$ solutions with 15 mM of DIC and seven different $[Mg^{2+}]$ ranging from 2.78 μM to 106.4 mM at various pH levels. The averaged $\delta^{13}C_{BaCO_3}$ values for these sets of experiments with distinct $[Mg^{2+}]$ were within $\pm 0.5\%$ of the $\delta^{13}C$ value of the $NaHCO_3$ (Table 2).

The results from the experiments with relatively low $[Mg^{2+}]$ ranging from 2.78 μM to 2.5 mM were generally similar to the control experiments. The average yields for these experimental series were essentially 100% ($\pm 3.2\%$ at most) relative to the expected yield (Table 2). This is consistent with the fact that the XRD profiles of the representative samples from solutions with $[Mg^{2+}]$ up to 2.5 mM showed no evidence of mineral formation other than $BaCO_3$ (Fig. 2). Fig. 4 shows that the $\alpha_{BaCO_3-H_2O}$ data from these low $[Mg^{2+}]$ experiments are mostly situated within the 95% confidence interval associated with the statistical fitting of the Mg^{2+} -free control results to the theoretical curve of α_{S-H_2O} as a function of pH by Zeebe (2007).

The experiments with much higher $[Mg^{2+}]$ of 26.6 mM to 106.4 mM showed quite different characteristics. Preparation of the parent solutions for these experiments had to be limited to pH < 8 because solutions prepared at higher pH values always resulted in spontaneous precipitation of white solids in the solutions (most likely $Mg(OH)_2$, see Fig. 2). The average sample yield for the experimental series at $[Mg^{2+}]$ of 26.6 mM, 53.2 mM and 106.4 mM was $130.4 \pm 4.0\%$, $162.5 \pm 16.7\%$ and $142.8 \pm 21.4\%$, respectively (Table 2). The excess yields reflect co-precipitation of $BaCO_3$ and $Mg(OH)_2$ in the sample. More importantly, the $\delta^{18}O_{BaCO_3}$ and hence $\alpha_{BaCO_3-H_2O}$ data from replicate samples were extremely inconsistent in these high $[Mg^{2+}]$ experiments (Fig. 5). This was never observed for the results from the control experiments and the experiments with $[Mg^{2+}]$ less than 2.5 mM (see Figs. 3 and 4). Because of poor reproducibility, the results from the experiments with high $[Mg^{2+}]$ of 26.6 to 106.4 mM were rejected.

3.4. Constant $[Mg^{2+}]$ experiments

For these experiments, quantitative precipitations were performed from the parent solutions with constant $[Mg^{2+}]$ of 2.5 mM and variable [DIC] ranging from 1.86 mM to 15 mM. The experimental results are summarized in Table S3 (Supplementary materials). In Fig. 6, the $\alpha_{BaCO_3-H_2O}$ data from the control and the constant $[Mg^{2+}]$ experiments are compared. The figure essentially shows no clear statistical difference between the results from the constant $[Mg^{2+}]$ experiments and the control experiments.

One concern for these experiments was increased susceptibility of the samples to contamination at low [DIC]. Note that we manipulated [DIC] of the parent solutions by adding different amounts of $NaHCO_3$. Decreasing [DIC] in the parent solutions leads to less production of $BaCO_3$ originating from the source $NaHCO_3$. This means that the contribution of small amounts of contaminants (e.g., from absorption of

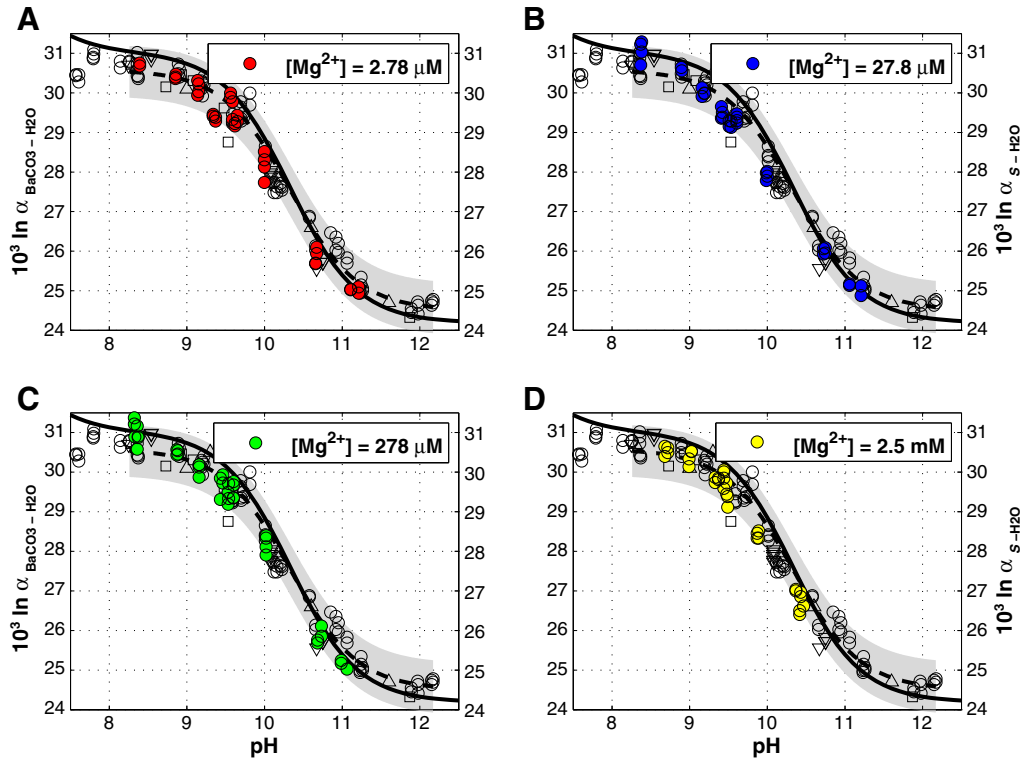


Fig. 4. Comparison of the $\alpha_{\text{BaCO}_3\text{-H}_2\text{O}}$ data obtained from the Mg^{2+} -free control experiments (open symbols) and from the variable $[\text{Mg}^{2+}]$ experiments (filled circles). The results from four sets of experiments with relatively low $[\text{Mg}^{2+}]$ concentrations up to 2.5 mM are displayed here (see Table 2). (Panel A) Control experiments versus 2.78 μM $[\text{Mg}^{2+}]$ experiments (red circles); (Panel B) control versus 27.8 μM $[\text{Mg}^{2+}]$ experiments (blue circles); (Panel C) control versus 278 μM $[\text{Mg}^{2+}]$ experiments (green circles); (Panel D) control versus 2.5 mM $[\text{Mg}^{2+}]$ experiments (yellow circles). See the Fig. 3 legend for the data compilation from Mg^{2+} -free experiments displayed here. The dashed curve and shaded area indicate the best fit curve for the results from the Mg^{2+} -free control experiments and the 95% confidence interval associated with the statistical fit, respectively.

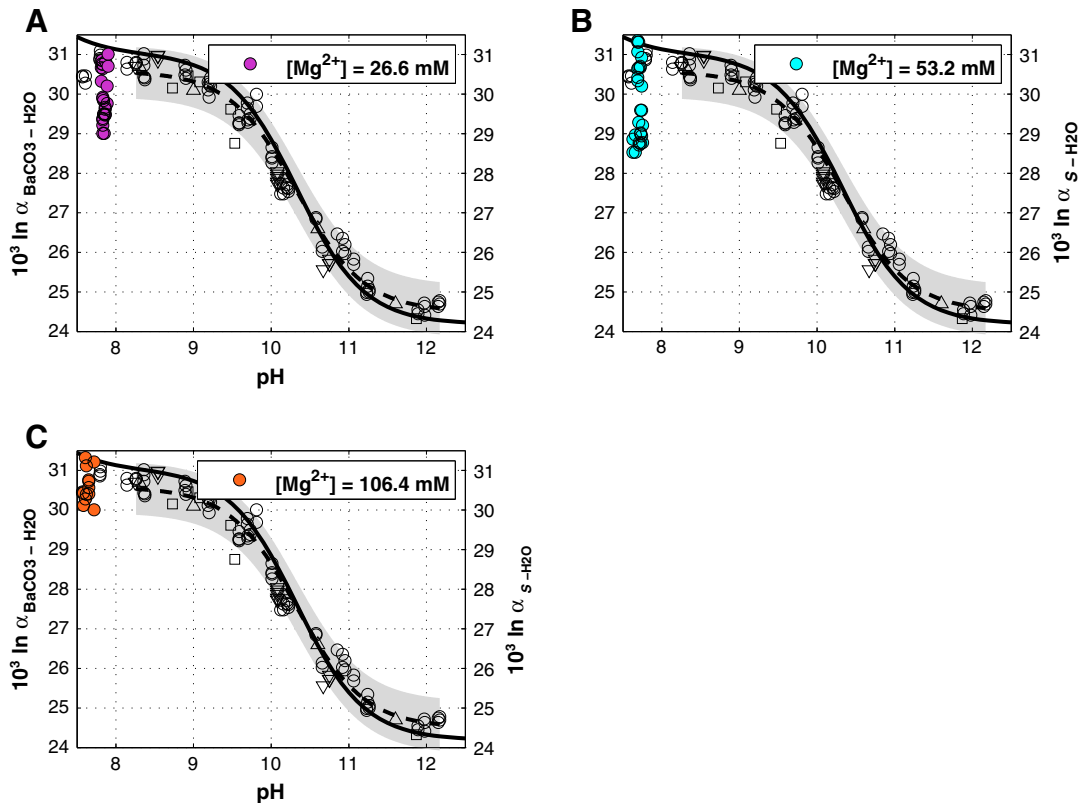


Fig. 5. The same as Fig. 4, but with the results from the variable $[\text{Mg}^{2+}]$ experiments performed at $[\text{Mg}^{2+}]$ of 26.6 mM (Panel A), at 53.2 mM (Panel B) and at 106.4 mM (Panel C). Note that the $[\text{Mg}^{2+}]$ in seawater is approximately 54 mM.

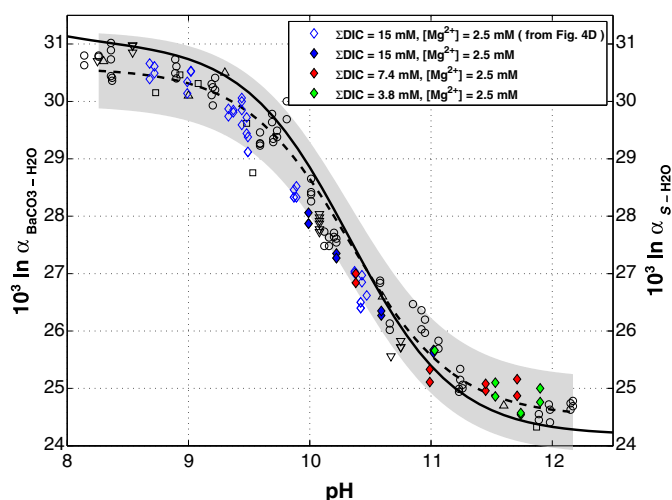


Fig. 6. Comparison of the $\alpha_{\text{BaCO}_3\text{-H}_2\text{O}}$ data obtained from the Mg-free control experiments (open symbols) and from the constant $[\text{Mg}^{2+}]$ experiments performed at $[\text{Mg}^{2+}]$ of 2.5 mM and variable [DIC] (filled symbols). (Blue diamonds) Experiments at [DIC] of 15 mM. (Red diamonds) Experiments at [DIC] of 7.4 mM. (Green diamonds) Experiments at [DIC] of 3.8 mM. The data shown by the open blue diamonds are the experimental results presented in Fig. 4D (variable $[\text{Mg}^{2+}]$ experiments at [DIC] of 15 mM and $[\text{Mg}^{2+}]$ of 2.5 mM). The dashed curve and shaded area indicate the best fit curve for the results from the Mg^{2+} -free control experiments and the 95% confidence interval for predictions based on the statistical fit, respectively.

ambient CO_2) becomes progressively more evident at lower [DIC]. Hence, filtration of these samples was performed under N_2 -atmosphere to circumvent absorption of atmospheric CO_2 . For the experiments at [DIC] of 3.75 to 15 mM, the sample $\delta^{13}\text{C}_{\text{BaCO}_3}$ values agreed with the $\delta^{13}\text{C}_{\text{NaHCO}_3}$ value within 0.7‰ on average. But for the experiments at [DIC] of 1.86 mM, the average disparity between the $\delta^{13}\text{C}_{\text{BaCO}_3}$ and $\delta^{13}\text{C}_{\text{NaHCO}_3}$ values was as large as 1.3‰, indicating more serious contamination issues for these particular samples. This suggests that CO_2 absorption during filtration is not the only source of contamination (see Uchikawa and Zeebe (2012) for other possibilities). The results from the experiments performed at [DIC] of 1.86 mM were rejected because of sample contamination.

4. Discussion

4.1. Sample rejection and assessment for quantitative BaCO_3 precipitation

Because of inconsistent $\delta^{18}\text{O}_{\text{BaCO}_3}$ and $\alpha_{\text{BaCO}_3\text{-H}_2\text{O}}$ data, which is accompanied by $\text{Mg}(\text{OH})_2$ co-precipitation, the results from the experiments with $[\text{Mg}^{2+}]$ higher than 2.5 mM were rejected (Fig. 5 and Table 2). The results from the constant $[\text{Mg}^{2+}]$ experiments with [DIC] of 1.86 mM were also rejected due to the $\delta^{13}\text{C}$ evidence of contamination (Table 2). Accordingly, the samples accepted for the following discussion are limited to those from the variable $[\text{Mg}^{2+}]$ experiments with $[\text{Mg}^{2+}]$ up to 2.5 mM and from the constant $[\text{Mg}^{2+}]$ experiments with [DIC] from 3.75 to 15 mM.

For the purpose of this study, a critical requirement is that the BaCO_3 samples were “quantitatively” precipitated from the parent solutions. A useful indicator for the quantitative precipitation is the sample $\delta^{13}\text{C}_{\text{BaCO}_3}$ values. Because the NaHCO_3 used for the preparation of the parent solutions represents the only carbon source for BaCO_3 samples, there must be reasonable agreement between the $\delta^{13}\text{C}_{\text{BaCO}_3}$ and $\delta^{13}\text{C}_{\text{NaHCO}_3}$ values upon successful quantitative precipitation. In our previous study based on very similar quantitative BaCO_3 experiments (Uchikawa and Zeebe, 2012), we rejected the experimental results unless the sample $\delta^{13}\text{C}_{\text{BaCO}_3}$ values agreed with the $\delta^{13}\text{C}_{\text{NaHCO}_3}$ values within 0.5‰. Such cut-off threshold was mandatory because the

majority of the precipitation experiments were not replicated in that study. But this is not the case for the present study where at least two chemically very similar parent solutions were prepared as the replicate. In this study, some of the accepted BaCO_3 samples showed the $\delta^{13}\text{C}$ offset exceeding $\pm 0.5\%$. Nevertheless their $\delta^{18}\text{O}_{\text{BaCO}_3}$ values were consistent among the replicate samples (ignoring the rejected samples described above). Thus, the $\delta^{13}\text{C}$ -based sample screening for the accepted samples was not applied here.

4.2. Synthesis of experimental results

Within the limit of $[\text{Mg}^{2+}]$ of 2.5 mM, the relative abundance of MgCO_3^0 in $[\text{CO}_3^{2-}]_{\text{T}}$ and in [DIC] was varied over 0 to ~40% and 0 to ~36%, respectively. Despite such chemical manipulations, the $\delta^{18}\text{O}_{\text{BaCO}_3}$ and $\alpha_{\text{BaCO}_3\text{-H}_2\text{O}}$ values obtained from the experiments with Mg^{2+} -addition and Mg^{2+} -free control experiments were not significantly different (Figs. 4 and 6).

In Fig. 7, the experimentally derived $\alpha_{\text{S-H}_2\text{O}}$ (note that $\alpha_{\text{BaCO}_3\text{-H}_2\text{O}} = \alpha_{\text{S-H}_2\text{O}}$) values are expressed in terms of their deviations from the best fit curve for the results from the control experiments (see Section 3.2 for detail). The results from our control experiments and those from McCrea (1950), Beck et al. (2005) and Kim et al. (2006) are generally in agreement within the 95% confidence interval based on our curve fitting (roughly ± 0.65 in $10^3 \ln \alpha_{\text{S-H}_2\text{O}}$ at pH levels above 8.2) as shown in Fig. 7A. Hence the range of ± 0.65 in $10^3 \ln \alpha_{\text{S-H}_2\text{O}}$ should be considered as a realistic experimental uncertainty for quantitative carbonate precipitations from simple $\text{Na}^+\text{-CO}_2\text{-H}_2\text{O}$ systems. Fig. 7C reiterates that the experimental results show no statistically significant difference regardless of the presence and concentrations of Mg^{2+} (up to 2.5 mM) in the parent NaHCO_3 solutions over the entire pH range tested in the present study. The dip in the $\Delta 10^3 \ln \alpha_{\text{S-H}_2\text{O}}$ data from the experiments with Mg^{2+} addition around pH 10 (although almost entirely within the experimental uncertainty) is probably an artifact. We suspect that this is due to the effect of Mg^{2+} on the second dissociation constant of carbonic acid (not included in our calculation), which sets the $[\text{HCO}_3^-]/[\text{CO}_3^{2-}]$ ratio and therefore the inflection point on the curve of $\alpha_{\text{S-H}_2\text{O}}$ as a function of pH (Zeebe, 2007). Fig. 7B shows no apparent trend between the $\Delta 10^3 \ln \alpha_{\text{S-H}_2\text{O}}$ and the relative abundance of MgCO_3^0 in $[\text{CO}_3^{2-}]_{\text{T}}$. In contrast, a comparison of the $\Delta 10^3 \ln \alpha_{\text{S-H}_2\text{O}}$ data with the MgCO_3^0 abundance in [DIC] reveals a subtle increasing trend starting from the MgCO_3^0 /[DIC] ratio of 10% (Fig. 7D). However, the data with negative $\Delta 10^3 \ln \alpha_{\text{S-H}_2\text{O}}$ between the MgCO_3^0 /[DIC] ratio of 10% and 20% in Fig. 7D corresponds to the ones situated in the dip around pH 10 in Fig. 7B. Hence, we argue that the positive shift in the $\Delta 10^3 \ln \alpha_{\text{S-H}_2\text{O}}$ values with the increase in MgCO_3^0 /[DIC] (Fig. 7D) also reflects an experimental artifact, which is explained by the ionic influence on the second dissociation constant of carbonic acid, and hence cannot be attributed to the effect of MgCO_3^0 complex formation on the equilibrium oxygen isotope fractionation factors $\alpha_{\text{HCO}_3\text{-H}_2\text{O}}$ and $\alpha_{\text{CO}_3\text{-H}_2\text{O}}$.

4.3. Applicability of the equilibrium fractionation factors by Beck et al. (2005) to seawater

Garrels and Thompson (1962) and Kester and Pytkowicz (1969) suggested that MgCO_3^0 accounts for 67% of $[\text{CO}_3^{2-}]_{\text{T}}$ inventory in seawater at 25 °C. Since these pioneering studies, improvements were made on the characterization of the activity coefficients for the ionic species in seawater (Pytkowicz and Hawley, 1974) and the dissociation constant $K_{\text{MgCO}_3}^0$ (Siebert and Hostetler, 1997b). Revised estimates by Pytkowicz and Hawley (1974) and Siebert and Hostetler (1997b) demonstrate that roughly 44% of $[\text{CO}_3^{2-}]_{\text{T}}$ in seawater is complexed as MgCO_3^0 at 25 °C, which means that the MgCO_3^0 abundance in [DIC] in typical surface seawater is only on the order of 4%. This is consistent with the numerical solution for the ion speciation in seawater at 25 °C using a more recent PHREEQ aqueous geochemical model (Parkhurst

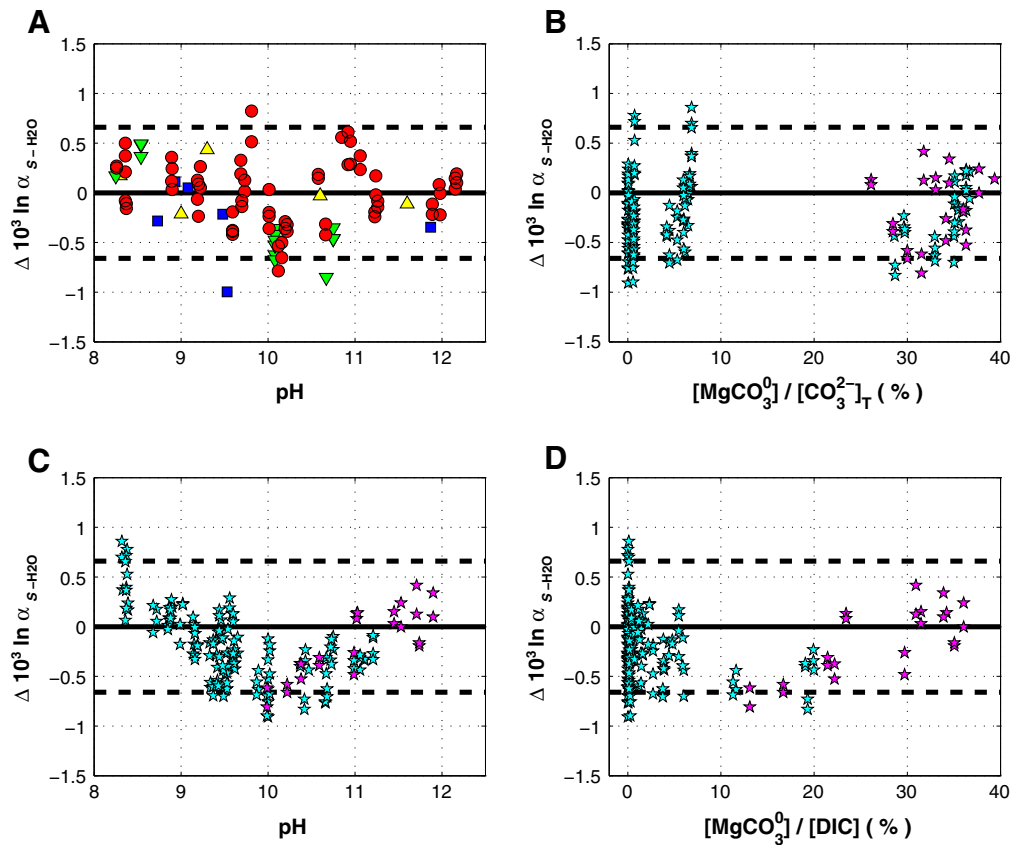


Fig. 7. Comparison of the empirically-derived and theoretically-calculated α_{S-H_2O} values. The $\Delta 10^3 \alpha_{S-H_2O}$ values refer to the deviations of the experimental $10^3 \alpha_{S-H_2O}$ values from the best fit curve for the results from the control experiments. Dashed lines indicate the 95% confidence interval for predictions based on the curve fitting. (Panel A) The $\Delta 10^3 \alpha_{S-H_2O}$ values for the control experiments (yellow upward triangles: McCrea (1950), blue squares: Beck et al. (2005), green downward triangles: Kim et al. (2006), red circles: this study). (Panels B, C and D) The $\Delta 10^3 \alpha_{S-H_2O}$ values for the experiments with Mg^{2+} -additions. Cyan stars represent the accepted results from the variable $[Mg^{2+}]$ experiments and magenta stars indicate the results from the constant $[Mg^{2+}]$ experiments.

and Appelo, 1999). On the contrary, the relative abundance of $MgCO_3^0$ complex in [DIC] was varied from 0 to 36% within the limit of $[Mg^{2+}]$ of 2.5 mM in our experiments. These data support the relevance of our experimental results to seawater, albeit the fact that the highest $[Mg^{2+}]$ achieved in our successful experiments is unfortunately about 20 times less than the average value in typical seawater. Based on the evidence from our experiments, the complex formation between Mg^{2+} and CO_3^{2-} (also HCO_3^-) appears to have a negligible influence on the ^{18}O equilibrium in the CO_2 - H_2O system. While Na^+ is another important agent for complex formation with CO_3^{2-} and HCO_3^- (Garrels and Thompson, 1962; Kester and Pytkowicz, 1969; Pytkowicz and Hawley, 1974), Beck et al. (2005) experimentally demonstrated that complex formation by Na^+ is likewise negligible on the ^{18}O equilibrium. These lines of evidence suggest that the ionic interactions such as ion pairing and complex formation do not compromise the applicability of the freshwater-based equilibrium oxygen isotope fractionation in the CO_2 - H_2O system (namely $\alpha_{HCO_3-H_2O}$ and $\alpha_{CO_3-H_2O}$) by Beck et al. (2005) in natural seawater.

4.4. Challenges for quantitative carbonate precipitation with Mg^{2+}

Undoubtedly, quantitative carbonate precipitation experiments using natural or artificial seawater would provide the most reliable information to evaluate whether the freshwater-based fractionation factors can be applied to seawater. However, we argue that such experiments are extremely difficult (and most probably impractical) considering the strong ionic interactions and possible interferences on the carbonate precipitation process. We focused on the effect of Mg^{2+} as it represents the most important cation for complexation of CO_3^{2-} in

seawater (Garrels and Thompson, 1962; Kester and Pytkowicz, 1969; Pytkowicz and Hawley, 1974; Siebert and Hostetler, 1997b). But even simple Mg^{2+} addition alone was problematic. Typical [DIC] and $[Mg^{2+}]$ of the average surface seawater are roughly on the order of 2.2 mM and 54 mM, respectively. Our results suggest that the experiments at such conditions would be of little use as there will be significant interference due to co-precipitation of $Mg(OH)_2$ (see Fig. 5).

Co-precipitation of $Mg(OH)_2$ with $BaCO_3$ is undesirable in two ways. First, it slows down the sample filtration process considerably. The size of $Mg(OH)_2$ particles formed from Mg^{2+} -containing alkaline solutions at low temperatures can be as small as 100 to 200 nm (Lv et al., 2004; Qian et al., 2007). The formation of superfine $Mg(OH)_2$ particles appears to be the primary cause for sluggish filtration, which increases the probability of sample contamination by absorption of ambient CO_2 (e.g., Bishop, 1990) unless proper precautions for filtration are taken (see Methods). The thermodynamic solubility product (K_{sp}) from the literature range from $10^{-11.20}$ to $10^{-10.50}$ for $Mg(OH)_2$ and from $10^{-8.80}$ to $10^{-8.56}$ for $BaCO_3$ (Pokrovsky and Schott, 2004; Busenberg and Plummer, 1986; and references therein), indicating that $Mg(OH)_2$ is even less soluble in H_2O compared to $BaCO_3$. Rinsing the precipitates with a generous volume of H_2O should have little to no effect on co-precipitated $Mg(OH)_2$. Once formed, it appears unfeasible to selectively eliminate $Mg(OH)_2$ without affecting $BaCO_3$.

Secondly, if the $Mg(OH)_2$ abundance relative to $BaCO_3$ in samples crosses a certain threshold, $Mg(OH)_2$ appears to interfere with $\delta^{18}O$ measurements. This is exemplified by the results from experiments with $[Mg^{2+}]$ from 26.6 to 106.4 mM (Fig. 5). Despite no $\delta^{13}C$ evidence of sample contamination, the $\delta^{18}O_{BaCO_3}$ values (and $\alpha_{BaCO_3-H_2O}$ values) of these samples were highly inconsistent. Although we do

not have definitive evidence, we suspect that the observed inconsistency in $\delta^{18}\text{O}_{\text{BaCO}_3}$ values may have to do with the possible reaction of $\text{Mg}(\text{OH})_2$ with H_3PO_4 during isotopic analyses.

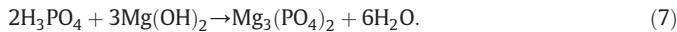
The H_3PO_4 used for the isotopic analyses of carbonate samples is prepared to a specific gravity of 1.93 g/cm^3 (supersaturation of 103–105%), typically by dissolving excess P_2O_5 to the 85% H_3PO_4 solution (e.g., Coplen et al., 1983). The reaction between H_3PO_4 and a given carbonate mineral (BaCO_3 for example) is expressed as:



This reaction produces CO_2 (to be analyzed on a mass spectrometer) as well as H_2O . Wachter and Hayes (1985) experimentally demonstrated that the $\delta^{18}\text{O}$ values of the CO_2 can be altered toward more negative values due to the oxygen isotope exchange with H_2O in reaction vessels. As summarized in Burman et al. (2005), the use of supersaturated H_3PO_4 prepared with excess P_2O_5 can circumvent this problem essentially by titrating H_2O :



$\text{Mg}(\text{OH})_2$ that co-exists in BaCO_3 samples may react with H_3PO_4 as follows:



The resultant H_2O could overwhelm the titration capacity of P_2O_5 . Furthermore, the $\delta^{18}\text{O}$ value of co-precipitated $\text{Mg}(\text{OH})_2$ can be very low because OH^- is depleted in ^{18}O by ~41‰ with respect to H_2O (Usdowski and Hoefs, 1993). Consequently, the H_2O formed from the possible reaction between $\text{Mg}(\text{OH})_2$ and H_3PO_4 (Eq. (7)) should be very depleted in ^{18}O as well. The oxygen isotope exchange between CO_2 (liberated from BaCO_3) and H_2O that is depleted in ^{18}O (liberated from $\text{Mg}(\text{OH})_2$) may ultimately explain the inconsistency in $\delta^{18}\text{O}$ measurements. However, an additional experimental study is required to evaluate this hypothesis.

5. Conclusion

We examined the possible effect of Mg^{2+} ions in solution on the equilibrium oxygen isotope fractionation in the CO_2 – H_2O system based on quantitative BaCO_3 precipitation experiments. The results of BaCO_3 precipitations from simple NaHCO_3 solutions prepared at various pH values (control experiments) were in accordance with the data from three independent studies. Under our experimental conditions, the upper limit of $[\text{Mg}^{2+}]$ to avoid undesirable interference on $\delta^{18}\text{O}$ measurements by excessive co-precipitation of $\text{Mg}(\text{OH})_2$ was 2.5 mM. Within this limit, the abundance of MgCO_3^0 in $[\text{CO}_3^{2-}]_{\text{T}}$ and [DIC] was varied over a 0 to 40% and 0 to 36% range, respectively. Nevertheless, the $\alpha_{\text{BaCO}_3\text{-H}_2\text{O}}$ values were invariant regardless of the abundance of MgCO_3^0 complexes in the parent solutions. Note that Mg^{2+} represents the most important cation for complex formation with dissolved CO_2 species in seawater. Thus, the outcome from this study suggests that the ionic interactions (including ion pairing and complex formation) do not compromise the applicability of freshwater equilibrium oxygen isotope fractionation factors in the CO_2 – H_2O system ($\alpha_{\text{HCO}_3\text{-H}_2\text{O}}$ and $\alpha_{\text{CO}_3\text{-H}_2\text{O}}$, Beck et al. (2005)) to environmental waters including natural seawater.

Acknowledgments

We are indebted to Howie Spero, Dave Winter and Lael Vetter (Univ. of California Davis) for stable isotope analyses and Ken Morris, Shantha Amarasinghe and Rahul Haware (Univ. of Hawaii Hilo) for XRD analyses. J. Uchikawa thanks his dissertation committee (Brian Popp, Yuan-Hui Li, Gregory Ravizza and Jane Schoonmaker) for their valuable comments.

We also thank Uwe Brand for editorial handling and two anonymous referees, whose reviews significantly improved this manuscript. This research was supported by the U.S. NSF awards (OCE05-25647 and OCE09-27089). This is SOEST contribution #8879.

Appendix A

Interactions of the dissolved ionic constituents in the parent solutions were modeled by a scheme similar to that of Garrels and Thompson (1962). The CO_3^{2-} speciation in the parent solutions containing Na^+ and Mg^{2+} can be described by the following mass-balance equations:

$$[\text{DIC}] = [\text{CO}_{2(\text{aq})}] + [\text{HCO}_3^-]_{\text{T}} + [\text{CO}_3^{2-}]_{\text{T}} \quad (\text{A} - 1)$$

$$[\text{HCO}_3^-]_{\text{T}} = [\text{HCO}_3^-]_{\text{F}} + [\text{MgHCO}_3^+] + [\text{NaHCO}_3^0] \quad (\text{A} - 2)$$

$$[\text{CO}_3^{2-}]_{\text{T}} = [\text{CO}_3^{2-}]_{\text{F}} + [\text{MgCO}_3^0] + [\text{NaCO}_3^-] \quad (\text{A} - 3)$$

where the subscripts T and F denote the total and free ion concentration, respectively. These equations can be combined to yield:

$$[\text{DIC}] = [\text{CO}_{2(\text{aq})}] + [\text{HCO}_3^-]_{\text{F}} + [\text{MgHCO}_3^+] + [\text{NaHCO}_3^0] + [\text{CO}_3^{2-}]_{\text{F}} + [\text{MgCO}_3^0] + [\text{NaCO}_3^-]. \quad (\text{A} - 4)$$

The activity of an ion is related to its concentration by the activity coefficient (γ). For example, in case of CO_3^{2-} ions:

$$\{\text{CO}_3^{2-}\} = \gamma_{\text{CO}_3^{2-}} \cdot [\text{CO}_3^{2-}]_{\text{F}}. \quad (\text{A} - 5)$$

Square brackets and curly brackets denote concentration in mol/kg and activity, respectively. Hence, (Eq. (A-4)) can be expressed in terms of activities of the respective ionic species:

$$[\text{DIC}] = \frac{\{\text{CO}_2\}}{\gamma_{\text{CO}_2}} + \frac{\{\text{HCO}_3^-\}}{\gamma_{\text{HCO}_3^-}} + \frac{\{\text{MgHCO}_3^+\}}{\gamma_{\text{MgHCO}_3^+}} + \frac{\{\text{NaHCO}_3^0\}}{\gamma_{\text{NaHCO}_3^0}} + \frac{\{\text{CO}_3^{2-}\}}{\gamma_{\text{CO}_3^{2-}}} + \frac{\{\text{MgCO}_3^0\}}{\gamma_{\text{MgCO}_3^0}} + \frac{\{\text{NaCO}_3^-\}}{\gamma_{\text{NaCO}_3^-}}. \quad (\text{A} - 6)$$

To solve Eq. (A-6) for $\{\text{CO}_3^{2-}\}$, a set of thermodynamic equilibrium constants are required:

$$\text{CO}_2 + \text{H}_2\text{O} \leftrightarrow \text{HCO}_3^- + \text{H}^+ \quad (\text{A} - 7)$$

$$K_1^\circ = \{\text{HCO}_3^-\} \cdot \{\text{H}^+\} / \{\text{CO}_2\} = 4.69 \times 10^{-11}$$

$$\text{HCO}_3^- \leftrightarrow \text{CO}_3^{2-} + \text{H}^+ \quad (\text{A} - 8)$$

$$K_2^\circ = \{\text{CO}_3^{2-}\} \cdot \{\text{H}^+\} / \{\text{HCO}_3^-\} = 4.45 \times 10^{-7}$$

$$\text{MgHCO}_3^+ \leftrightarrow \text{Mg}^{2+} + \text{HCO}_3^- \quad (\text{A} - 9)$$

$$K_{\text{MgHCO}_3^+}^\circ = \{\text{Mg}^{2+}\} \cdot \{\text{HCO}_3^-\} / \{\text{MgHCO}_3^+\} = 8.5 \times 10^{-2}$$

$$\text{NaHCO}_3^0 \leftrightarrow \text{Na}^+ + \text{HCO}_3^- \quad (\text{A} - 10)$$

$$K_{\text{NaHCO}_3^0}^\circ = \{\text{Na}^+\} \cdot \{\text{HCO}_3^-\} / \{\text{NaHCO}_3^0\} = 1.78$$

$$\text{MgCO}_3^0 \leftrightarrow \text{Mg}^{2+} + \text{CO}_3^{2-} \quad (\text{A} - 11)$$

$$K_{\text{MgCO}_3^0}^\circ = \{\text{Mg}^{2+}\} \cdot \{\text{CO}_3^{2-}\} / \{\text{MgCO}_3^0\} = 10.47 \times 10^{-4}$$

$$\text{NaCO}_3^- \leftrightarrow \text{Na}^+ + \text{CO}_3^{2-} \quad (\text{A} - 12)$$

$$K_{\text{NaCO}_3^-}^\circ = \{\text{Na}^+\} \cdot \{\text{CO}_3^{2-}\} / \{\text{NaCO}_3^-\} = 5.37 \times 10^{-2}.$$

The numerical values for these constants are calculated at 25 °C. The first and second dissociation constants of carbonic acid (K°_1 and K°_2) are from [Plummer and Busenberg \(1982\)](#). The stability constants $K^{\circ}_{\text{MgHCO}_3^-}$ and $K^{\circ}_{\text{MgCO}_3^0}$ are from [Siebert and Hostetler \(1997a, 1997b\)](#). The constants $K^{\circ}_{\text{NaHCO}_3^0}$ and $K^{\circ}_{\text{NaCO}_3^-}$ are from [Garrels and Thompson \(1962\)](#).

Using the equilibrium relationships above and re-arranging Eq. (A-6):

$$\begin{aligned} \{\text{CO}_3^{2-}\} = & [\text{DIC}] / \left(\left(\frac{\{\text{H}^+\}^2}{\gamma_{\text{CO}_2} \cdot K^{\circ}_1 \cdot K^{\circ}_2} \right) + \left(\frac{\{\text{H}^+\}}{\gamma_{\text{HCO}_3^-} \cdot K^{\circ}_2} \right) \right. \\ & + \left(\frac{\{\text{Mg}^{2+}\} \{\text{H}^+\}}{\gamma_{\text{MgHCO}_3^-} \cdot K^{\circ}_{\text{MgHCO}_3^-}} \right) + \left(\frac{\{\text{Na}^+\} \{\text{H}^+\}}{\gamma_{\text{NaHCO}_3^0} \cdot K^{\circ}_{\text{NaHCO}_3^0}} \right) \\ & + \left(\frac{\{\text{Mg}^{2+}\}}{\gamma_{\text{MgCO}_3^0} \cdot K^{\circ}_{\text{MgCO}_3^0}} \right) + \left(\frac{\{\text{Na}^+\}}{\gamma_{\text{NaCO}_3^-} \cdot K^{\circ}_{\text{NaCO}_3^-}} \right) \\ & \left. + \left(\frac{1}{\gamma_{\text{CO}_3^{2-}}} \right) \right). \end{aligned} \quad (\text{A-13})$$

The input variables [DIC], $[\text{Mg}^{2+}]$, $[\text{Na}^+]$ and $[\text{H}^+]$ (for calculating the activity of the respective ions in Eq. (A-13)) can be constrained from the NaHCO_3 , MgCl_2 and NaOH added to the parent solutions and from the pH measurements (for calculation of activity coefficients, see below). Once $\{\text{CO}_3^{2-}\}$ is calculated, the following relationship can be used to calculate $[\text{MgCO}_3^0]$ and $[\text{NaCO}_3^-]$:

$$\{\text{MgCO}_3^0\} = \frac{\{\text{Mg}^{2+}\} \cdot \{\text{CO}_3^{2-}\}}{K^{\circ}_{\text{MgCO}_3^0}} \quad \text{and} \quad [\text{MgCO}_3^0] = \frac{\{\text{MgCO}_3^0\}}{\gamma_{\text{MgCO}_3^0}} \quad (\text{A-14})$$

and

$$\{\text{NaCO}_3^-\} = \frac{\{\text{Na}^+\} \cdot \{\text{CO}_3^{2-}\}}{K^{\circ}_{\text{NaCO}_3^-}} \quad \text{and} \quad [\text{NaCO}_3^-] = \frac{\{\text{NaCO}_3^-\}}{\gamma_{\text{NaCO}_3^-}}. \quad (\text{A-15})$$

Finally, quantities such as $[\text{MgCO}_3^0]/[\text{CO}_3^{2-}]_{\text{T}}$ and $[\text{MgCO}_3^0]/[\text{DIC}]$ (see Fig. 7) were calculated.

Activity coefficients for dissolved ions were calculated by the extended Debye–Hückel equation following [Siebert and Hostetler \(1997b\)](#) because of the similarity in the range of ionic strength (I) tested in their experiments and in the experiments from which our accepted BaCO_3 samples were produced:

$$\log(\gamma) = A z^2 \left(\frac{\sqrt{I}}{1 + B a \sqrt{I}} \right). \quad (\text{A-13})$$

The numerical value for the constants A and B at 25 °C in water is 0.5085 and 0.3281×10^8 , respectively. The ion size parameters (a) are from [Siebert and Hostetler \(1997b\)](#). For uncharged dissolved CO_2 , $\gamma_{\text{CO}_2} = 1$ was assigned ([Garrels and Thompson, 1962](#)). In addition, we assumed $\gamma_{\text{MgCO}_3^0} = 1.13$, $\gamma_{\text{NaHCO}_3^0} = 1.13$ and $\gamma_{\text{NaCO}_3^-} = 0.68$ from [Garrels and Thompson \(1962\)](#). [Reardon and Langmuir \(1976\)](#) established an empirical expression for $\gamma_{\text{MgCO}_3^0}$ as a function of ionic strength at 25 °C. But the use of $\gamma_{\text{MgCO}_3^0}$ by [Reardon and Langmuir \(1976\)](#) in exchange for $\gamma_{\text{MgCO}_3^0} = 1.13$ by [Garrels and Thompson \(1962\)](#) caused negligible differences in the final outcomes of the calculation within the range of ionic strength tested in this study.

Appendix B. Supplementary data

Supplementary data to this article can be found online at <http://dx.doi.org/10.1016/j.chemgeo.2013.02.002>.

References

- Adkins, J.F., Boyle, E.A., Curry, W.B., Lutringer, A., 2003. Stable isotopes in deep-sea corals and a new mechanism for 'vital effects'. *Geochimica et Cosmochimica Acta* 67, 1129–1143.
- Allison, N., Finch, A.A., EIMF, 2010. The potential origins and paleoenvironmental implications of high temporal resolution $\delta^{18}\text{O}$ heterogeneity in coral skeletons. *Geochimica et Cosmochimica Acta* 74, 5537–5548.
- Beck, W.C., Grossman, E.L., Morse, J.W., 2005. Experimental studies of oxygen isotope fractionation in the carbonic acid system at 15° 25° and 40 °C. *Geochimica et Cosmochimica Acta* 69, 3493–3503.
- Bemis, B.E., Spero, H.J., Bijma, J., Lea, D.W., 1998. Reevaluation of the oxygen isotopic composition of planktonic foraminifera: experimental results and revised paleotemperature equations. *Paleoceanography* 13, 150–160. <http://dx.doi.org/10.1029/98PA00070>.
- Bishop, P.K., 1990. Precipitation of dissolved carbonate species from natural water for $\delta^{13}\text{C}$ analysis – a critical appraisal. *Chemical Geology* 80, 251–259.
- Böttcher, M.E., 1996. $^{18}\text{O}/^{16}\text{O}$ and $^{13}\text{C}/^{12}\text{C}$ fractionation during the reaction of carbonates with phosphoric acid: effects of cationic substitution and reaction temperature. *Isotopes in Environmental and Health Studies* 32, 299–305.
- Brennkmeijer, C.A.M., Kraft, P., Mook, W.G., 1983. Oxygen isotope fractionation between CO_2 and H_2O . *Chemical Geology* 41, 181–190.
- Burman, J., Gustafsson, O., Segl, M., Schmitz, B., 2005. A simplified method of preparing phosphoric acid for stable isotope analyses of carbonates. *Rapid Communications in Mass Spectrometry* 19, 3086–3088.
- Busenberg, E., Plummer, L.N., 1986. The solubility of $\text{BaCO}_3(\text{cr})$ (witherite) in CO_2 – H_2O solutions between 0 and 90 °C, evaluation of the association constants of $\text{BaHCO}_3^+(\text{aq})$ and $\text{BaCO}_3^0(\text{aq})$ between 5 and 80 °C, and a preliminary evaluation of the thermodynamic properties of $\text{Ba}^{2+}(\text{aq})$. *Geochimica et Cosmochimica Acta* 50, 2225–2233.
- Coplen, T.B., Kendall, C., Hoppfe, J., 1983. Comparison of stable isotope reference samples. *Nature* 320, 236–238.
- Cramer, B.S., Toggweiler, J.R., Wright, J.D., Katz, M.E., Miller, K.G., 2009. Ocean overturning since the Late Cretaceous: inferences from a new benthic foraminiferal isotope compilation. *Paleoceanography* 24, PA4216. <http://dx.doi.org/10.1029/2008PA001683>.
- Curry, W.B., Duplessy, J.C., Labeyrie, L.D., Shackleton, N.J., 1988. Changes in the distribution of $\delta^{13}\text{C}$ of deep water $\sum \text{CO}_2$ between the Last Glaciations and the Holocene. *Paleoceanography* 3, 317–341.
- Das Sharma, S., Patil, D.T., Gopalan, K., 2002. Temperature dependence of oxygen isotope fractionation of CO_2 from magnetite–phosphoric acid reaction. *Geochimica et Cosmochimica Acta* 66, 589–593.
- Dickens, G.R., O'Neil, J.R., Rea, D.K., Owen, R.M., 1995. Dissociation of oceanic methane hydrate as a cause of the carbon isotope excursion at the end of the Paleocene. *Paleoceanography* 10, 956–971. <http://dx.doi.org/10.1029/95PA02087>.
- Epstein, S., Mayeda, T., 1953. Variation of O^{18} content of waters from natural sources. *Geochimica et Cosmochimica Acta* 4, 213–224.
- Epstein, S., Buchsbaum, R., Lowenstam, H., Urey, H.C., 1953. Revised carbonate-water isotopic temperature scale. *Geological Society of America Bulletin* 64, 1315–1326.
- Friedrich, O., Norris, R.D., Erbacher, J., 2012. Evolution of middle to Late Cretaceous oceans – a 55 m.y. record of Earth's temperature and carbon cycle. *Geology* 40, 107–110.
- Garrels, R.M., Thompson, M.E., 1962. A chemical model for sea water at 25 °C and one atmosphere total pressure. *American Journal of Science* 260, 57–66.
- Grossman, E.L., Ku, T.-L., 1986. Oxygen and carbon isotope fractionation in biogenic aragonite-temperature effects. *Chemical Geology* 59, 59–74.
- Halas, S., Wolaciewicz, W., 1982. The experimental study of oxygen isotope exchange reaction between dissolved bicarbonate and water. *Journal of Chemical Physics* 76, 5470–5472.
- JCPDS, 1974. Selected powder diffraction data for minerals – data book. Joint Committee on Powder Diffraction Standards. (Swarthmore, Pennsylvania).
- Kennett, J.P., Cannariato, K.G., Hendsy, I.L., Behl, R.J., 2000. Carbon isotope evidence for methane hydrate instability during Quaternary Interstadials. *Science* 208, 128–133.
- Kester, D.R., Pytkowicz, R.M., 1969. Sodium, magnesium, and calcium sulfate ion-pairs in seawater at 25 °C. *Limnology and Oceanography* 14, 686–692.
- Kim, S.-T., O'Neil, J.R., 1997. Equilibrium and nonequilibrium oxygen isotope effects in synthetic carbonates. *Geochimica et Cosmochimica Acta* 61, 3461–3475.
- Kim, S.-T., Hillaire-Marcel, C., Mucci, A., 2006. Mechanisms of equilibrium and kinetic oxygen isotope effects in synthetic aragonite at 25 °C. *Geochimica et Cosmochimica Acta* 70, 5790–5801.
- Kim, S.-T., Mucci, A., Taylor, B.E., 2007a. Phosphoric acid fractionation factors for calcite and aragonite between 25 and 75 °C: revisited. *Chemical Geology* 246, 135–146.
- Kim, S.-T., O'Neil, J.R., Hillaire-Marcel, C., Mucci, A., 2007b. Oxygen isotope fractionation between synthetic aragonite and water: influence of temperature and Mg^{2+} concentration. *Geochimica et Cosmochimica Acta* 71, 4704–4715.
- Lisiecki, L.E., Raymo, M.E., 2005. A Pliocene–Pleistocene stack of 57 globally distributed benthic $\delta^{18}\text{O}$ records. *Paleoceanography* 20, PA1003. <http://dx.doi.org/10.1029/2004PA001071>.
- Lv, J., Qiu, L., Qu, B., 2004. Controlled growth of three morphological structures of magnesium hydroxide nanoparticles by wet precipitation method. *Journal of Crystal Growth* 267, 676–684.
- McConnaughey, T.A., 2003. Sub-equilibrium oxygen-18 and carbon-13 levels in biological carbonates: carbonate and kinetic models. *Coral Reefs* 22, 316–327.
- McCrea, J.M., 1950. On the isotopic chemistry of carbonates and a paleotemperature scale. *Journal of Chemical Physics* 18, 849–853.

- Mook, W.G., 1986. ^{13}C in atmospheric CO_2 . *Netherlands Journal of Sea Research* 20, 211–223.
- Morse, J.W., Wang, Q., Tsio, M.Y., 1997. Influences of temperature and Mg:Ca ratio on CaCO_3 precipitates from seawater. *Geology* 25, 85–87.
- Oppo, D.W., Linsley, B.K., Rosenthal, Y., Dannenmann, S., Beaufort, L., 2003. Orbital and suborbital climate variability in the Sulu Sea, western tropical Pacific. *Geochemistry, Geophysics, Geosystems* 4, 1003. <http://dx.doi.org/10.1029/2001GC000260>.
- Paneth, P., O'Leary, M.H., 1985. Carbon isotope effect on dehydration of bicarbonate ion catalyzed by carbonic anhydrase. *Biochemistry* 24, 5143–5147.
- Parkhurst, D.L., Appelo, C.A.J., 1999. User's guide to PHREEQC (version 2) – a computer program for speciation, batch-reaction, one-dimensional transport, and inverse geochemical calculations. U.S. Geological Survey, Water-Resources Investigations Report 99-4259.
- Plummer, L.N., Busenberg, E., 1982. The solubilities of calcite, aragonite and vaterite in CO_2 - H_2O solutions between 0 and 90 °C, and an evaluation of the aqueous model for the system CaCO_3 - CO_2 - H_2O . *Geochimica et Cosmochimica Acta* 46, 1011–1040.
- Pokrovsky, O.S., Schott, J., 2004. Experimental study of brucite dissolution and precipitation in aqueous solutions: surface speciation and chemical affinity control. *Geochimica et Cosmochimica Acta* 68, 31–45.
- Pytkowicz, R.M., Hawley, J.E., 1974. Bicarbonate and carbonate ion-pairs and a model of seawater at 25 °C. *Limnology and Oceanography* 19, 223–234.
- Qian, H.-Y., Deng, M., Zhang, S.-M., Xu, L.-L., 2007. Synthesis of superfine $\text{Mg}(\text{OH})_2$ particles by magnesite. *Materials Science and Engineering: A* 445–446, 600–603.
- Reardon, E.C., Langmuir, D., 1976. Activity coefficients of MgCO_3^0 and CaSO_4^0 ion pairs as a function of ionic strength. *Geochimica et Cosmochimica Acta* 40, 549–554.
- Rollion-Bard, C., Chaussidon, M., France-Lanord, C., 2003. pH control on oxygen isotopic composition of symbiotic corals. *Earth and Planetary Science Letters* 215, 275–288.
- Romanek, C.S., Grossman, E.L., Morse, J.W., 1992. Carbon isotope fractionation in synthetic aragonite and calcite: effects of temperature and precipitation rate. *Geochimica et Cosmochimica Acta* 56, 419–430.
- Sharma, T., Clayton, R.N., 1965. Measurement of $\text{O}^{18}/\text{O}^{16}$ of total oxygen of carbonates. *Geochimica et Cosmochimica Acta* 29, 1347–1353.
- Siebert, R.M., Hostetler, P.N., 1997a. The stability of the magnesium bicarbonate ion pair from 10° to 90 °C. *American Journal of Science* 277, 697–715.
- Siebert, R.M., Hostetler, P.B., 1997b. The stability of the magnesium carbonate ion pair from 10° to 90 °C. *American Journal of Science* 277, 716–734.
- Spero, H.J., Bijma, J., Lea, D.W., Bemis, B.E., 1997. Effect of seawater carbonate concentration on foraminiferal carbon and oxygen isotopes. *Nature* 390, 497–500.
- Thode, H.G., Shima, M., Rees, C.E., Krishnamurty, K.V., 1965. Carbon-13 isotope effects in systems containing carbon dioxide, bicarbonate, carbonate and metal ions. *Canadian Journal of Chemistry* 43, 582–595.
- Uchikawa, J., Zeebe, R.E., 2012. The effect of carbonic anhydrase on the kinetics and equilibrium of the oxygen isotope exchange in the CO_2 - H_2O system: implications for $\delta^{18}\text{O}$ vital effects in biogenic carbonates. *Geochimica et Cosmochimica Acta* 95, 15–34.
- Urey, H.C., 1947. The thermodynamic properties of isotopic substances. *Journal of the Chemical Society* 562–581.
- Uzdowski, E., Hoefs, J., 1993. Oxygen isotope exchange between carbonic acid, bicarbonate, carbonate, and water: a re-examination of the data of McCrea (1950) and an expression for the overall partitioning of oxygen isotopes between the carbonate species and water. *Geochimica et Cosmochimica Acta* 57, 3815–3818.
- Wachter, E.A., Hayes, J.M., 1985. Exchange of oxygen isotopes in carbon dioxide-phosphoric acid system. *Chemical Geology* 52, 365–374.
- Zachos, J.C., Pagani, M., Sloan, L., Thomas, E., Billups, K., 2001. Trends, rhythms, and aberrations in global climate 65 Ma to present. *Science* 291, 1511–1517.
- Zachos, J.C., Dickens, G.R., Zeebe, R.E., 2008. An early Cenozoic perspective on greenhouse warming and carbon-cycle dynamics. *Nature* 451, 279–283.
- Zeebe, R.E., 1999. An explanation of the effect of seawater carbonate concentration on foraminiferal oxygen isotopes. *Geochimica et Cosmochimica Acta* 63, 2001–2007.
- Zeebe, R.E., 2007. An expression for the overall oxygen isotope fractionation between the sum of dissolved inorganic carbon and water. *Geochemistry, Geophysics, Geosystems* 8, Q09002. <http://dx.doi.org/10.1029/2007GC001663>.
- Zeebe, R.E., Sanyal, A., 2002. Comparison of two potential strategies of planktonic foraminifera for house building: Mg^{2+} or H^+ removal? *Geochimica et Cosmochimica Acta* 66, 1159–1169.
- Zeebe, R.E., Wolf-Gladrow, D., 2001. CO_2 in Seawater: Equilibrium, Kinetics, Isotopes. Elsevier Oceanography Series, vol. 65. Elsevier, Amsterdam.
- Zhang, J., Quay, P.D., Wilbur, D.O., 1995. Carbon isotope fractionation during gas-water exchange and dissolution of CO_2 . *Geochimica et Cosmochimica Acta* 59, 107–114.